2516–2530 *Nucleic Acids Research, 2017, Vol. 45, No. 5* *Published online 9 December 2016*
doi: 10.1093/nar/gkw1212

And-1 coordinates with CtIP for efficient homologous recombination and DNA damage checkpoint maintenance

Yali Chen[1,†], Hailong Liu[1,†], Haoxing Zhang[2,†], Changqing Sun[3,†], Zhaohua Hu[4], Qingsong Tian[4], Changmin Peng[5], Pei Jiang[1], Hui Hua[1], Xinzhi Li[4] and Huadong Pei[1,*]

[1]State Key Laboratory of Proteomics, Beijing Proteome Research Center, Beijing Institute of Radiation Medicine, Beijing 100850, China, [2]School of Life Sciences and Oceanography, Shenzhen University, Shenzhen, Guangdong Province 518060, China, [3]Department of neurosurgery, Tianjin Baodi Hospital, Baodi Clinical College of Tianjin Medical University, Tianjin 301800, China, [4]Department of Orthopedics, Renhe Hospital of Three Gorges University, Yichang 443001, China and [5]Key Laboratory of Industrial Fermentation Microbiology, Ministry of Education, Tianjin Industrial Microbiology Key Lab, College of Biotechnology, Tianjin University of Science and Technology, No 29, 13ST. TEDA, Tianjin 300457, China

Received July 22, 2016; Revised November 17, 2016; Editorial Decision November 18, 2016; Accepted November 25, 2016

ABSTRACT

To prevent genomic instability, cells respond to DNA lesions by blocking cell cycle progression and initiating DNA repair. Homologous recombination repair of DNA breaks requires CtIP-dependent resection of the DNA ends, which is thought to play a key role in activation of CHK1 kinase to induce the cell cycle checkpoint. But the mechanism is still not fully understood. Here, we establish that And-1, a replisome component, promotes DNA-end resection and DNA repair by homologous recombination. Mechanistically, And-1 interacts with CtIP and regulates CtIP recruitment to DNA damage sites. And-1 localizes to sites of DNA damage dependent on MDC1-RNF8 pathway, and is required for resistance to many DNA-damaging and replication stress-inducing agents. Furthermore, we show that And-1-CtIP axis is critically required for sustained ATR–CHK1 checkpoint signaling and for maintaining both the intra-S- and G2-phase checkpoints. Our findings thus identify And-1 as a novel DNA repair regulator and reveal how the replisome regulates the DNA damage induced checkpoint and genomic stability.

INTRODUCTION

DNA double-strand breaks (DSBs) are most dangerous for genomic integrity, and it is critically important for cells to detect and properly repair them to prevent neoplastic transformation (1–3). Cells are equipped with a network of interacting pathways known as the DNA damage response (DDR), to detect and correct these breaks (1,4–7). This response coordinates DNA repair with cell cycle checkpoint controls. DSBs induce cell cycle arrest in G1 and G2 phases as well as slowing down of DNA synthesis (8–10). Checkpoints allow time for DSB repair, which is mediated by either homologous recombination (HR) or nonhomologous end joining (NHEJ) (11–13).

NHEJ is active in all phases of the cell cycle, and HR in eukaryotic cells is regulated during the cell cycle to occur most efficiently during the S and G2 phases when sister chromatids are present. The Mre11/Rad50/Nbs1 (MRN) complex binds to DSB ends and plays important roles in initiating HR-mediated DSB repair (14–17). CtIP (CtBP-interacting protein), which is associated with MRN and BRCA1, is also a critical player in the regulation of HR (8,18–22). We and others report that USP4 interacts with CtIP and the MRE11–RAD50–NBS1 (MRN) complex and is required for CtIP recruitment to DNA damage sites and DNA end resection (23,24). The Mre11 subunit possesses the catalytic function of MRN complex in resection and has both 5′-flap endonuclease activity and 3′→5′ exonuclease activity. Its endonuclease function is believed to initiate resection by internal cleavage of the 5′ strand to generate oligonucleotides that will be released, while the exonuclease activity processes the resulting 3′ ends on the DNA. The end resection also needs other proteins, such as CtIP, BLM, EXO1, DNA2 and the recently described EXD2 and EEPD1 (25–30). Some groups showed that CtIP also exhibits 5′-flap endonuclease activity on branched DNA structures, independent of the MRN complex. And the nuclease activity of CtIP is specifically required for the removal

*To whom correspondence should be addressed. Tel: +86 10 80701533; Fax: +86 10 80701533; Email: peihuadong@hotmail.com
†These authors contributed equally to this work as first authors.

of DNA adducts at sites of DNA breaks (31,32). The ssDNA generated from the resection process is immediately coated by replication protein A (RPA), which promotes HR repair (33,34).

Various studies suggest that CtIP and its homologues in various organisms are required for DNA damage checkpoint maintenance (8,22,35,36). CtIP is important for DNA end resection. After DNA end resection, RPA-coated ssDNA is bound by ATRIP which leads to ATR activation and downstream CHK1 activation. CHK1 is required for the S- and G2-phase checkpoints in mammalian cells (37), and its activity is regulated by ATR phosphorylation on S317 and S345 (4). Thus, CtIP can regulate DNA end resection and ssDNA generation, and promote ATR mediated CHK1 phosphorylation and S- and G2-phase checkpoints (8,19,35). But the regulating mechanism is still not fully understood.

CtIP is directly phosphorylated by cyclin-dependent kinases (CDKs) (38). CDK-mediated phosphorylation of CtIP on T847 is required to promote resection, whereas CDK-dependent phosphorylation of CtIP-S327 during G2 phase of the cell cycle is required for interaction with BRCA1 (8,20,39). In chicken DT40 cells, mutation of CtIP-S327 into a nonphosphorylatable residue inhibits HR repair (20). In mammalian cells, CtIP–BRCA1 complex formation facilitates removal of 53BP1 binding protein RIF1 from DSB regions (40). BRCA1 and 53BP1 act antagonistically to regulate DNA end resection. 53BP1 inhibits DNA end resection through its associated factors RIF1 and pax transactivation domain interacting protein (PTIP) (40,41). However, the physiological role of CtIP–BRCA1 binding has been questioned by the finding that knock-in mice homozygous for CtIP-S326A allele are neither tumor-prone or HR deficient (42,43).

Here, we report that acidic nucleoplasmic DNA-binding protein 1 (And-1), a replisome component (44–46), regulates DNA repair and cellular survival upon DSB induction. We also show that And-1 depletion impairs HR repair by affecting the process of DNA-end resection. Additionally, we found that And-1 interacts with CtIP and that these interactions are required for DNA damage checkpoint maintenance, thereby linking DNA processing with prolonged cell cycle arrest to allow sufficient time for DNA repair.

MATERIALS AND METHODS

Cell culture and transfection

U2OS, MCF-7, HEK-293T, HCC1937 cells were purchased from ATCC. HEK-293T, MCF-7 and U2OS cells were cultured in DMEM supplemented with 10% FBS at 37°C with 5% CO_2. HCC1937 cells were cultured in RPMI1640 supplemented with 15% FBS at 37°C with 5% CO_2. All transfections were conducted using Lipofectamine 2000 (Invitrogen) according to the manufacturer's instructions.

Antibodies and constructs

And-1 antibody was obtained from Novus (#NBP1-89091, dilution: 1:500 for WB and 1:100 for IF). BRCA1 (D-9, dilution: 1:100 for IF, Santa Cruz) and (C-20, 1:200 for WB and IP, Santa Cruz), HA (H9658, dilution: 1:1000 for WB and IP, Sigma), FLAG (F3165, dilution: 1:1000 for WB and IP, Sigma), γH2AX (05-636, dilution: 1:500 for IF, Millipore), CtIP (61141, dilution: 1:500, Active Motif) for IF and (sc-28324, dilution 1:11 000) for WB, Chk1 (sc-7898, dilution: 1:1000 for WB, Santa Cruz), and P-Chk1-317 (2344S, 1:500 for WB, Cell Signaling), MDC1 (ab11171, 1:500 for IF), NBS1(ab32074, 1:200 for IF) were used. Antibodies against RPA, RAD51 and 53BP1 were previously described (47–49). And-1 full-length was subcloned from pEFF-And-1(a kind gift from Dr Zhu) (44) into the Flag-tagged vector (pIRES2-EGFP) and HA-tagged vector (pCMV-HA) and GFP-tagged vector (pFUGW). And-1 deletion mutants were generated by site-directed mutagenesis and confirmed by sequencing. Full-length CtIP and D1–D6 deletion mutants were kindly provided by Dr Chen (50).

RNAi target sequences

SiRNAs were synthesized by Genepharma. For siRNA transfection, cells were transfected twice at 24-h interval with the indicated siRNA using Lipofectamine® RNAiMAX (Invitrogen) according to the manufacturer's instructions. The sequences of siRNAs against human AND-1 were: AAGCAGGCAUCUGCAGCAUCCdTdT, AGGAAAACAUGCCUGCCACdTdT (5′-UTR), and GGUGUAGGUAACAGGACAUdTdT (3′-UTR). The other siRNA sequences were: MDC1 (UCCAGUGAAUCCUUGAGGUdTdT), RNF8 (GGACAAUUAUGGACAACAAdTdT), NBS1 (GGCGUGUCAGUUGAUGAAAdTdT), CtIP (GCUAAAACAGGAACGAAUCdTdT), 53BP1 (GAGCUGGGAAGUAUAAAUUdTdT). The target sequence of shRNAs were as follows: human AND1 (AAGCAGGCATCTGCAGCATCC and GGTGTAGGTAACAGGACATAT), CtIP (CGGCAGCAGAATCTTAAACTT). For lentiviral infection, shRNA lentiviral particles were packaged and transduced into the indicated cells according to the manufacturer's guidelines (Sigma).

Tandem affinity purification (TAP)

HEK-293T cells stable transfected with SFB-tagged CtIP were established. Tandem Affinity Purification was performed. Breifly, cells were synchronized to S phase, irradiated (10 Gy, with a PXi X-RAD 160 X-ray Irradiator, at a dose rate of 1.907 Gy/min) and harvested 2 h later, then lysed in NETN buffer (20 mM Tris–HCl at pH 8.0, 100 mM NaCl, 1 mM EDTA, 0.5% Nonidet P-40) containing 10 mM NaF, and 1 μg/ml each of pepstatin A and aprotinin. Following centrifugation, the pellet was sonicated in high-salt solution (20 mM HEPES at pH 7.8, 0.4 M NaCl, 1 mM EDTA, 1 mM EGTA, protease inhibitors) to extract chromatin-bound proteins fractions. Then the chromatin extracts were incubated with streptavidin Sepharose beads (Amersham) for 4 h at 4°C. The immunocomplexes were washed three times with NETN buffer and eluted with NETN buffer containing 2 mg/ml biotin (Sigma). The eluates were incubated with S-protein agarose (Novagen) for 4 h at 4°C. After three washes, the immunocomplexes were separated by SDS-PAGE and visualized by Coomassie Blue staining.

Mass spectrometry

After staining proteins in SDS-PAGE gels with Coomassie blue, gel lanes were sliced into different bands and in-gel digested overnight at 37°C with trypsin. After digestion, peptides were extracted twice in 200 μl of acetonitrile with resuspension in 20 μl of 2% formic acid prior to second extraction, dried in a Savant SpeedVac, and dissolved in a 5% methanol/0.1% formic acid solution. Tryptic peptides were separated on a C18 column, and were analyzed by LTQ-Orbitrap Velos (Thermo). Proteins were identified by using the National Center for Biotechnology Information search engine against the human or mouse National Center for Biotechnology Information RefSeq protein databases.

Immunoprecipitation and GST-Pull down assay

Cells were lysed with NETN buffer containing protease inhibitors on ice for 30 min, then sonicated for 15 s. Following centrifugation, the clarified lysates were incubated with protein G or protein A agarose beads coupled with antibody against the indicated proteins for 8 h at 4°C. Beads were washed with NETN buffer three times and analyzed by western blot. For tagged protein IP, cell lysates were incubated with Anti-Flag M2 Affinity beads (Sigma) for 3 h at 4°C, or EZview™ Red anti-HA affinity beads (Sigma) for 8 h at 4°C. Precipitates were then washed and immunoblotted with the indicated antibodies. For the BRCA1 or CtIP GST-pull down assay, GST-BRCA1 fragments fusion proteins or GST-CtIP-N were expressed in *Escherichia coli*. Purified fusion proteins were immobilized on glutathione Sepharose 4B beads and incubated with cell lysates at 4°C. The samples were separated by SDS-PAGE and analyzed by western blot.

Laser microirradiation and imaging of cells

A Nikon A1R confocal system and a Coherent 405 nm laser unit was used. Briefly, the 405 nm laser microbeam is focused by a 60× (NA 1.4) oil immersion microscope objective. The total laser energy delivered to each focused spot was set by an attenuator plate and the number of pulses. U2OS cells transfected with indicated plasmid were plated on glass-bottomed culture dishes (MatTek) before laser irradiation. Cells were stained with Hoechst 33342 (10 μg/ml) for 70 min then exposed to the laser beam for about 15 s. Images were taken by the same microscope with Nikon NIS-Elements AR software (version 4.40.00). For quantitative and comparative imaging, signal intensities at the laser line were converted into a numerical value using the same AR software. To compensate for nonspecific fluorescent bleaching during the repeated image acquisition, in every image, we first measured the average fluorescent intensity (at the laser line) as a function of time and then divided it by the average fluorescent intensity measured elsewhere in the cell (background) as a function of time. To get normalized GFP-tagged proteins accumulation curve for each cell, the fluorescent intensity (RF) at the laser line was calculated by the following formula: $RF(t) = [(I - Ipre\ IR)/(Imax - Ipre\ IR)]$, where Ipre IR is the fluorescent intensity of the laser line region before irradiation and Imax represents the maximum fluorescent intensity at the laser line. Normalized fluorescent curves from four to six cells were averaged. The error bars represent the SD from the mean value. Signal intensities were plotted using Excel.

Immunofluorescence staining

Cells cultured on coverslips were treated with IR (5 or 10 Gy) followed by recovery for the indicated time. After washing with PBS, cells were fixed in 3% paraformaldehyde for 15 min and permeabilized in 0.5% triton X-100 solution for 5 min at room temperature. For And-1 staining, cells were pre-extracted for 5 min on ice in 25 mM HEPES (pH 7.4) buffer containing 0.5% Triton X-100, 50 mM NaCl, 1 mM EDTA, 3 mM $MgCl_2$ and 0.3 M sucrose, then fixed with 4% formaldehyde for 10 min at RT and permeabilized by soaking in 0.2% Triton X-100 for 5 min at RT. Cells were blocked with 5% goat serum and incubated with primary antibody for 60 min. Subsequently, samples were washed and incubated with secondary antibody for 30 min. DAPI staining was performed to visualize nuclear DNA. The coverslips were mounted onto glass slides and visualized by a Nikon ECLIPSE E800 fluorescence microscope.

Sensitivity to DNA damaging agents

HCT116 cells were transfected as indicated, plated onto 96-well plates and treated with MMC, Camptothecin, HU, IR or UV as indicated. Two days later, the viability of the cells was determined using the CellTiter-Blue reagent (Promega) and the average of four experiments was plotted. Data were presented as mean ± SD of three independent experiments.

DNA repair assay

Integrated DNA repair reporter systems were used to determine the HR and NHEJ efficiency. Briefly, HEK293 cells integrated with HR or NHEJ reporters were infected with the indicated viruses. Forty eight hours after infection, 4-hydroxytamoxifen (4-OHT) was added at 3 mM for 24 h to induce I-SecI expression. I-SecI is fused with an estrogen responsive element for inducible expression, and 4-OHT is an estrogen analog. Three days after 4-OHT was added, the percentage of GFP positive cells was analyzed by FACS. HR efficiency is presented as the percentage of control cells. Repair frequencies are the mean of at least three independent experiments and error bars represent the standard deviation from the mean value. Statistical analysis was performed by the Student's *t*-test for two groups and by ANOVA for multiple groups. $P < 0.05$ was considered significant.

G2/M checkpoint and intra-S checkpoint assay

For G2/M fraction, quantitating histone H3 phosphorylation was performed. Briefly, U2OS cells were transfected and IR treated as indicated. Nocodazole (1 μM, Sigma) was added 2 h after IR. Cells were fixed at indicated time post-IR, then stained with a phospho-H3S10 antibody and a Dylight488-conjugated secondary antibody sequentially. 50 μg/ml propidium iodide (Sigma) was added before

FACS analysis with FACS Calibur instrument (BD Biosciences). The bar chart shows the percentage of H3-S10p–positive cells. For intra-S checkpoint, RDS assay was performed. Briefly, U2OS cells transfected with the indicated siRNA. After 48 hours, cells were labeled with 10 nCi/ml of [^{14}C]thymidine (PerkinElmer Life Sciences) for 36 h to normalize the total amount of DNA, then irradiated with 10 Gy of IR and recovered for 1 h. Cells were then pulse-labeled with 1 μCi/ml [^{3}H]thymidine (PerkinElmer Life Sciences) for 30 min, washed with PBS, fixed with methanol, and lysed with 0.5 M NaOH. The lysates were counted in a liquid scintillation counter. RDS was calculated using the ratio of radioactivity of ^{3}H/^{14}C. Overlapping ^{3}H and ^{14}C emissions were corrected with quenched ^{3}H and ^{14}C standards. Data are the means of three independent experiments. Error bars represent SDs.

Flow cytometry

Cells were trypsinized and washed with PBS twice and centrifuged (800 rpm) at 4°C. Cells were fixed in 500 μl ice-cold 70% ethanol overnight at 4°C. Fixed cells were centrifuged at 500 rpm at 4°C for 10 min and suspended in 500 μl PBS containing 50 μg/ml propidium iodide (Sigma) and 10 μg/ml RNase for 30 min at 4°C. FACS analysis was performed with FACS Calibur instrument (BD Biosciences). ModFit (version 2.0) software was used for optimum analysis of cell cycle (G1, G2 and S phases).

Metaphase spread

Wild type MEFs were transfected with control or And-1 siRNA respectively. After 48 hours, metaphase spreading analysis of MEFs was performed. Briefly, cells were treated with Colcemid (100 ng/ml, Sigma) for 3 h before harvesting. After trypsinization, cells were washed once with PBS, then resuspended in 0.075 M KCl and incubated at 37°C for 30 min. After centrifugation, cells were fixed using a Carnoy's Fixative (75% methanol, 25% acetic acid) at RT for 10 min and then washed twice with fixative. Cells were resuspended in fixative and dropped onto slides. Slides were stained with 100 ng/ml DAPI solution (Sigma) for 5 min, then rinsed with PBS and air-dried. The images were recorded using a Nikon A1R confocal microscopy.

Statistical analysis

The statistical data are from three independent experiments. Statistical analysis was performed by the Student's *t*-test for two groups and by ANOVA (analysis of variance) for multiple groups. $P < 0.05$ was considered significant.

RESULTS

And-1 interacts with CtIP

To search for the partner of CtIP involved in HR, HEK-293T cells stably expressing SFB-tagged CtIP were arrested in S phase, CtIP purification was performed after ionizing radiation (IR) treatment, chromatin-associated CtIP complexes were isolated and subjected to mass spectrometry analysis. A number of known CtIP-associated proteins were co-purified, including BRCA1, USP4, SRCAP and Sirt6 (Figure 1A). To our surprise, we also identified And-1, a replisome component (45), as a CtIP interacting protein. And-1 is an important factor that functions together with HJURP to facilitate the cell cycle-specific recruitment of CENP-A to centromeres (45). It was also reported that And-1 coordinated with Claspin in response to replication stress (51). However, its role in DNA end resection is not clear. To further investigate this interaction, we examined whether And-1 and CtIP form a complex by a co-immunoprecipitation assay using chromatin-free cell extracts from HEK-293T cells. CtIP was readily detected in And-1 immunoprecipitates, vice versa (Figure 1B), suggesting that And-1 either interacts with CtIP, or these proteins associate with each other in a complex. And-1 contains WD40 repeats at its amino terminus, a SepB domain in the middle, and a HMG domain at its carboxyl terminus (44). We next tested which regions of And-1 are responsible for interacting with CtIP by expressing CtIP together with And-1 or its truncation mutants in HEK-293T cells (Figure 1C). And-1 deletion mutant (deletion residues 850–1050) abolished the binding of And-1 with CtIP. Similarly, we generated deletion mutants of CtIP (Figure 1D). The And-1-binding region of CtIP was mapped to the N terminal and C terminal (residues 17–160 and residues 732–892). A direct interaction between And-1 and the N terminal of CtIP expressed in *E.coli* was confirmed by GST pull down assay (Figure 1E). Interestingly, we also found that And-1-CtIP interaction is upregulated by DNA damage (Supplementary Figure S1A). As MRN complex interacted with CtIP, we tested whether And-1 can also interact with MRN complex. As shown in Supplementary Figure S1B, And-1 bound MRN complex weakly in cells.

And-1 localizes to sites of DNA damage

To explore the role of And-1 in the DDR, we investigated whether And-1 is recruited to sites of DNA damage. We expressed an N-terminal GFP-And-1 fusion protein in U2OS cells and assayed for its recruitment to DNA lesions induced by 405 nm laser microirradiation. The relocation kinetics of GFP-And-1 to DSBs was monitored in a time course as indicated. As shown in Figure 1F, And-1 showed a pan-nuclear staining in undamaged cells. However, within 2 min of microirradiation, And-1 was recruited to DNA damage sites where it colocalized with γH2AX, a marker of sites of DNA damage (Figure 1F and Supplementary Figure S1C). Furthermore, And-1 recruitment to DNA damage sites showed a similar kinetics as CtIP (Figure 1F and Supplementary Figure S1D). These findings suggest that perhaps And-1 directly functions in DNA damage response.

And-1 acts downstream of MDC1 and RNF8 following DNA damage

It is generally accepted that γH2AX-MDC1 is important for the chromatin response to DSBs. γH2AX-MDC1 is required for the sustained localization of a number of DNA damage mediator/repair factors at chromatin regions at or near the sites of DNA damage. To delineate where And-1 fits in the established DNA damage signaling cascade, we examined foci formation of And-1 in human cells with

A

CtIP purification

Protein	Peptide	Coverage(%)
CtIP	46	52.80
BRCA1	30	38.6
USP4	17	22.8
Sirt6	15	17.8
SRCAP	11	16.4
FAT10	9	30.68
And-1	8	10.1
HBXAP	8	9.2
PRPF8	7	6.8
PHF6	4	3.1

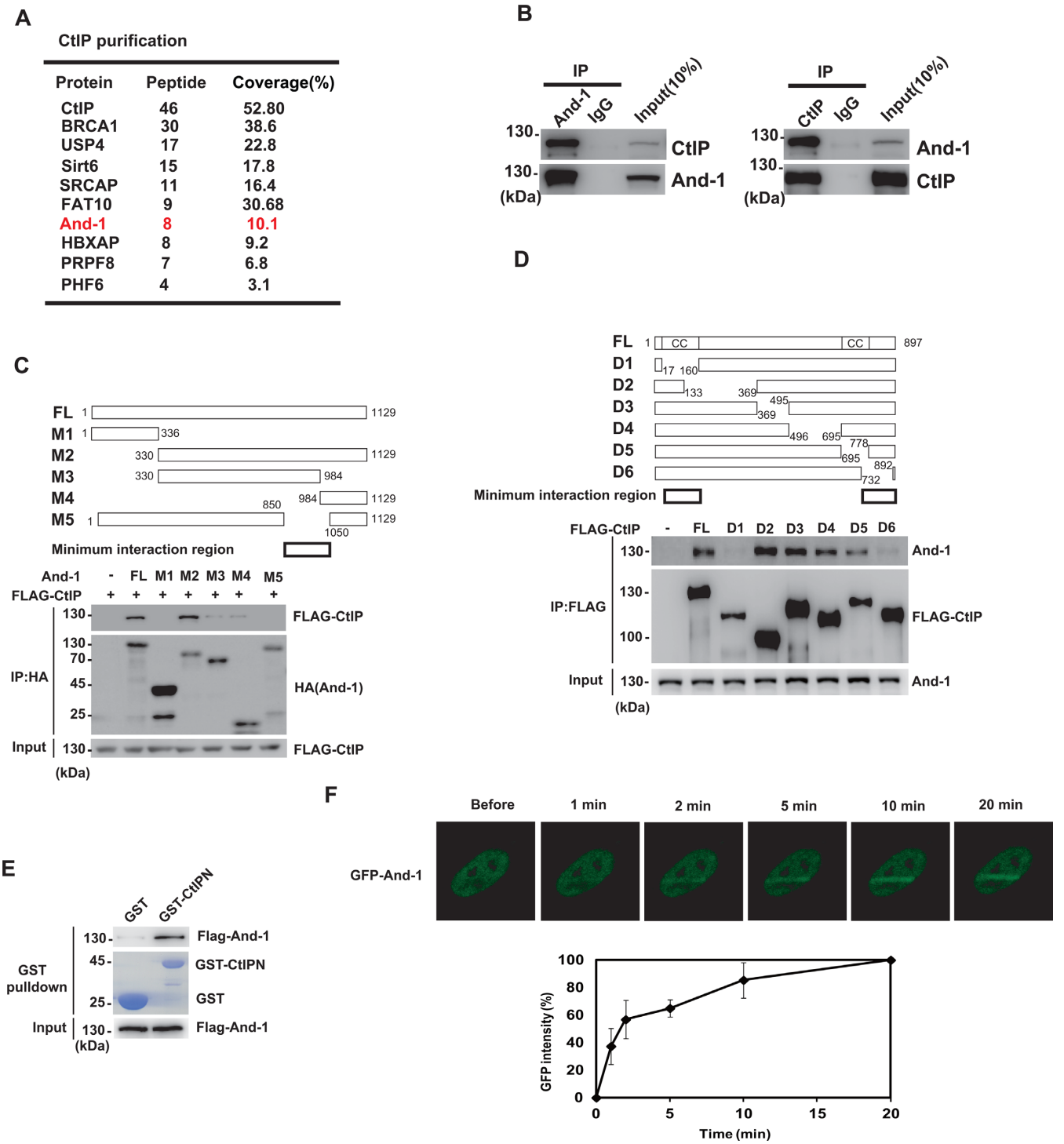

Figure 1. And-1 interacts with CtIP and localizes to sites of DNA Damage. (**A**) Tandem affinity purification was performed using HEK-293T cells stably expressing SFB-tagged CtIP as indicated in the method. The major hits from mass spectrometry analysis were shown in the table. (**B**) Co-immunoprecipitation (co-IP) assays were performed using U2OS cell lines to check the interaction between And-1 and CtIP. IPs were resolved by SDS–PAGE and immunoblotted for the indicated proteins. (**C**) Co-IP was performed to determine the regions essential for the CtIP-And-1 interaction. Upper panel, schematic representation of different And-1 mutants and the minimum interaction region. lower panel, HEK-293T cells were transiently transfected with the indicated constructs for 24 h. Cell lysates were immunoprecipitated with anti-HA affinity gel, and western blot was performed with indicated antibodies. (**D**) Co-IP was performed to determine the regions essential for the CtIP-And-1 interaction. Upper panel, schematic representation of CtIP constructs and the minimum interaction region. lower panel, HEK-293T cells were transiently transfected with the indicated constructs for 24 h. Cell lysates were immunoprecipitated with anti-Flag M2 affinity gel, and western blot was performed with indicated antibodies. (**E**) GST-pull-down assay of And-1 using the indicated proteins expressed in bacteria. (**F**) And-1 translocates to DNA damage sites upon DNA damage. U2OS cells transfected with GFP-And-1 were subjected to laser micro-irradiation to generate DSBs in a line pattern. The relocation kinetics of GFP-And-1 to DSBs was monitored in a time course as indicated. GFP intensities at the laser line were normalized into a numerical value using Nikon NIS-Elements AR software (version 4.40.00). Normalized fluorescent curves from 6 cells were averaged. The error bars represent SD.

knockout of various DNA damage response players. In contrast to the control cells, no IR-induced And-1 focus formation was observed in MDC1 or RNF8 deficient cells (Figure 2A and B). On the other hand, And-1 relocalization to γ-H2AX containing foci is not noticeably affected in cells with 53BP1 deficiency (Figure 2B). In the BRCA1-mutated breast cancer cell line, HCC1937 cells, And-1 focus formation was also decreased. When we put back wild type BRCA1 in HCC1937 cells, And-1 foci came back again (Figure 2C). These data suggest that perhaps And-1 acts downstream of MDC1 and RNF8 in the DNA damage responsive pathway. Given the results of BRCA1-dependent And-1 recruitment, we reasoned that And-1 might directly bind BRCA1. As shown in Figure 2D, indeed we found that endogenous BRCA1 associated with And-1, and this association was also DNA damage-inducible. BRCA1 contains BRCT domain at its C terminal which is responsible for protein-protein interactions (52–54). As shown in Figure 2E, we observed that And-1 could be pulled-down by the purified GST-BRCT (wild type) domain of BRCA1, but not by the BRCT (S1655A) mutant that is defective for binding to phospho-Ser/Thr motifs. But this interaction is indirect, as we could not find GST BRCT domain interacted with purified And-1 from cells after damage treatment (data not shown). To test whether the BRCT domain of BRCA1 is important for And-1 recruitment to DNA damage sites, we also detected And-1 foci formation in HCC1937 cells transfected with WT BRCA1 or the BRCA1 S1655A mutant. As shown in Figure 2F, And-1 foci formation was greatly decreased in BRCA1 S1655A-expressed cells than in WT BRCA1-expressed cells. Above results clearly indicated that And-1 recruitment depends on BRCA1 BRCT domain. In some recent documents, it has been reported a cell phase-specific BRCA1 recruitment (40,55). We further explored whether And-1 behaves similarly to BRCA1 upon DNA damage. As shown in Supplementary Figure S2A, the recruitment of And-1 to DSBs was mainly observed in S-phase cells.

Inactivation of and-1 sensitizes human cells to DNA damage and replication stress

Consistent with previous findings, we found that depletion of And-1 sensitized cells to HU and CPT in cancer cells (Figure 3A). In addition, similar to CtIP depletion, exposure of the cells to Etoposide, IR or UV also caused a reduction in the viability of cells depleted for And-1 (Figure 3A). To rule out off-target effects of the And-1 siRNA, we reconstituted And-1-depleted cells with an siRNA-resistant wild-type (WT) And-1 expression plasmid, and confirmed that the siRNA-resistant And-1 rescued the damage sensitivity conferred by the siRNA (Figure 3A). Next, we examined how And-1 regulates DNA repair using well-established reporter assays for HR and NHEJ (56). We found that And-1 depletion led to decreased HR frequency to a level similar to that achieved by depleting the key HR factor CtIP (Figure 3B). Conversely, we did not observe a so significant change in NHEJ frequency in And-1 knockdown cells (Figure 3C). And-1 depletion also rendered cells hypersensitive to PARP inhibitor (AZD2281) (Figure 3D), implying And-1′s important role in the HR pathway. Importantly, depletion of And-1 has no significant effect on cell-cycle distribution in U2OS cells without DNA damage, indicating that the effect of And-1 knockdown on HR was not caused by cell-cycle change (Supplementary Figure S2B). Furthermore, we found more chromosome aberrations in And-1 depleted cells than in control cells (Figure 3E), suggesting that And-1 plays a critical role in maintaining chromosome integrity.

And-1 promotes DNA end resection and the generation of ssDNA

CtIP is essential for efficient DNA end processing during DSB repair, with cells depleted for this factor showing a defect in the generation of ssDNA and the subsequent formation of RPA foci. Thus we hypothesized that And-1 may promote DNA end resection. To test this, we analysed RPA focus formation in response to IR in wild-type (WT) And-1 depleted cells. Strikingly, cells depleted for And-1 showed severely impaired RPA focus formation and single strand DNA production detected with BrdU staining in S/G2 phase (Figure 4A and Supplementary Figure S3A and B). DNA-end resection generates 3′ ssDNA tails that are coated by RPA. Subsequently, RAD51 is recruited to form a helical nucleoprotein filament (57). Consistent with a role of And-1 in HR, we observed that And-1 depletion resulted in sharply decreased Rad51 loading to DSBs (Figure 4B). As And-1 directly interacts with CtIP, we also checked CtIP foci formation in And-1 knocked down cells. As expected, depletion of And-1 dramatically inhibited CtIP foci formation in S/G2 phase (Figure 4C and Supplementary Figure S3C), but knockdown of CtIP did not affect And-1 foci formation (Supplementary Figure S3D). Meanwhile, the accumulation of upstream DNA damage repair factors (53BP1, BRCA1, MDC1, NBS1, RNF8, RNF168) at DSBs remained unperturbed (Figure 4D and E and Supplementary Figure S3E–H) in And-1 depleted cells. Previous studies also showed that MRN complex interacted with CtIP and regulated its recruitment. To test whether knockdown of And-1 affects the interaction between CtIP and MRN complex in S/G2 phase and whether And-1 and MRN work in the same pathway to recruit CtIP, we knocked down And-1 in HEK-293T cells, then checked MRN-CtIP interaction. As shown in Figure 4G, knockdown of And-1 did not affect the interaction between CtIP and MRN complex. We also found that double knockdown of And-1 and NBS1 showed stronger effect on CtIP recruitment than either single knockdown (Figure 4H). These results confirmed that And-1 and MRN did not work in the same pathway to recruit CtIP. Taken together, our results indicate that And-1 is a putative component of the resection machinery required for the efficient processing of DSBs.

And-1 regulates G2/M and intra S phase checkpoint

The generation of RPA-coated ssDNAs is also essential for CHK1 activation under genome stress. Indeed, And-1 knockdown decreased IR-induced CHK1 phosphorylation, but had no effect on CHK1 total level (Figure 5A). As CtIP has a critical role in the maintenance of the G2/M- and S-phase checkpoints, we next investigated the role of

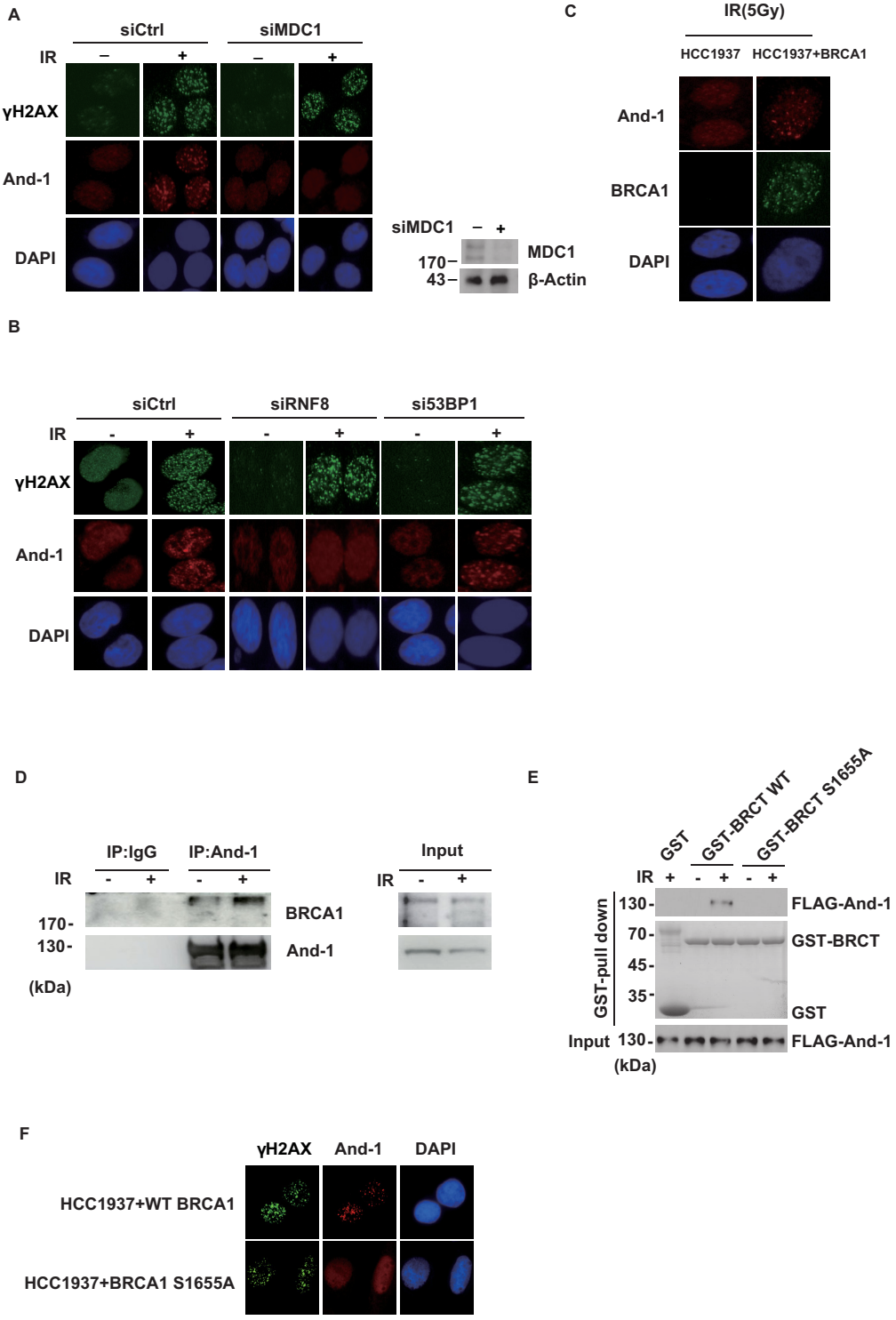

Figure 2. And-1 recruitment to DNA damage sites depends on MDC1-RNF8 pathway and BRCA1 BRCT domain. (**A**) And-1 accumulation at DSB sites requires MDC1. And-1 and γH2AX foci formation were examined in U2OS cells transfected with control or MDC1 siRNA following IR (10 Gy) treatment and 1-h recovery. Knock-down expression of MDC1 was examined. (**B**) And-1 accumulation at DSB sites requires RNF8 but not 53BP1. And-1 and γH2AX foci formation were examined in U2OS cells transfected with control or RNF8 or 53BP1 siRNA following IR (10 Gy) treatment. (**C**) And-1 recruitment to DNA damage sites depends on BRCA1. And-1 and BRCA1 foci formation were examined in HCC1937 and HCC1937+BRCA1 cells following IR (5 Gy) treatment and 1-h recovery. (**D**) Co-immunoprecipitation (co-IP) assays were performed to check the interaction between And-1 and BRCA1. HEK-293T Cells with or without IR (10 Gy) treatment were lysed and immunoprecipitated with IgG or And-1 antibody. (**E**) GST-pull-down assay of And-1 using wild-type BRCA1 BRCT domain or S1655A mutant. HEK-293T cells transfected with FLAG-And-1 were subjected to IR (10 Gy) treatment and 1-h recovery. Then the cell lysates were used for GST-pull-down assay. (**F**) And-1 recruitment to DNA damage sites depends on BRCA1 BRCT domain. HCC1937 cells were transfected with WT BRCA1 or BRCA1 S1655A mutant, then And-1 and γH2AX foci formation was examined following IR (5 Gy) treatment and 1-h recovery.

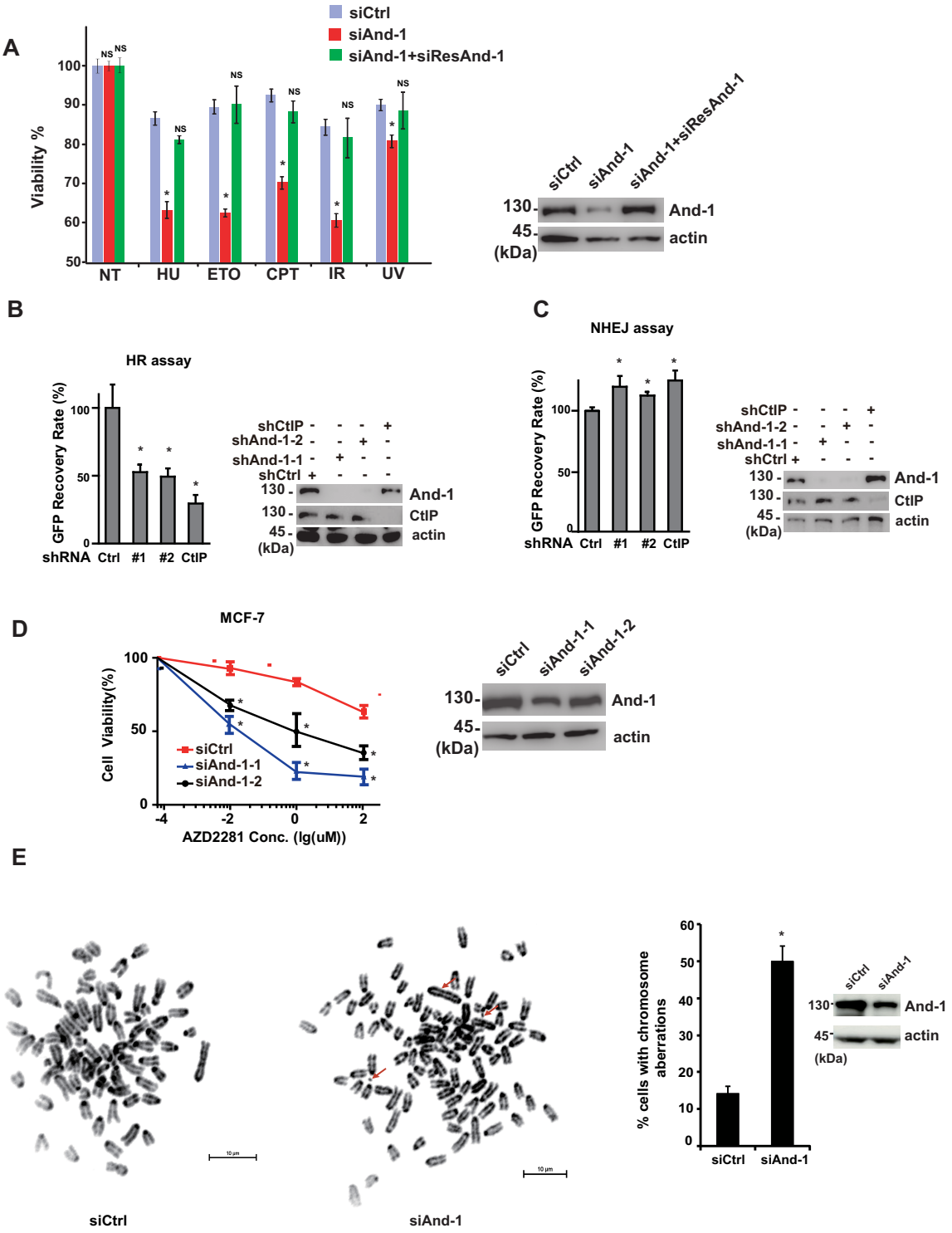

Figure 3. And-1 is involved in DNA damage response. (**A**) HCT116 cells were transfected with control or And-1 siRNA, then reconstituted with the indicated siRNA-resistant And-1. Sensitivity of cells to indicated DNA damage-inducing or replication stress-inducing agents was determined by MTS assays. Data were presented as mean ± SD of three biological triplicates. Expression of And-1 was examined. (**B** and **C**) HEK-293T cells integrated with NHEJ or HR reporter were infected with the indicated shRNA lentivirus and subjected to the HR assay (B) or NHEJ assay (C) as described in Methods. Data presented as mean ± SD of three biological triplicates. Positive cell percentage was compared with control group. $*P < 0.05$. (**D**) MCF-7 cells transfected with indicated siRNAs were treated with increasing doses of PARP inhibitor (AZD2281). MTS assay was performed to determine the surviving fraction. Data presented as mean ± SD of three biological triplicates. Surviving cell percentage was compared with control group. $*P < 0.05$. (**E**) Chromosome aberrations were induced by And-1 depletion. WT MEFs were transfected with control or And-1 siRNA. After 48 h, cells were treated with colcemid followed by mitotic spread staining. Left: representative images of mitotic spread in control and And-1 knockdown cells. Scale bar, 10 μm. Arrows, chromosome abberations. Right: quantification, the mean percentage of mitotic cells with four or more chromosome abberations. For each condition, 10 cells were counted. $*P < 0.05$.

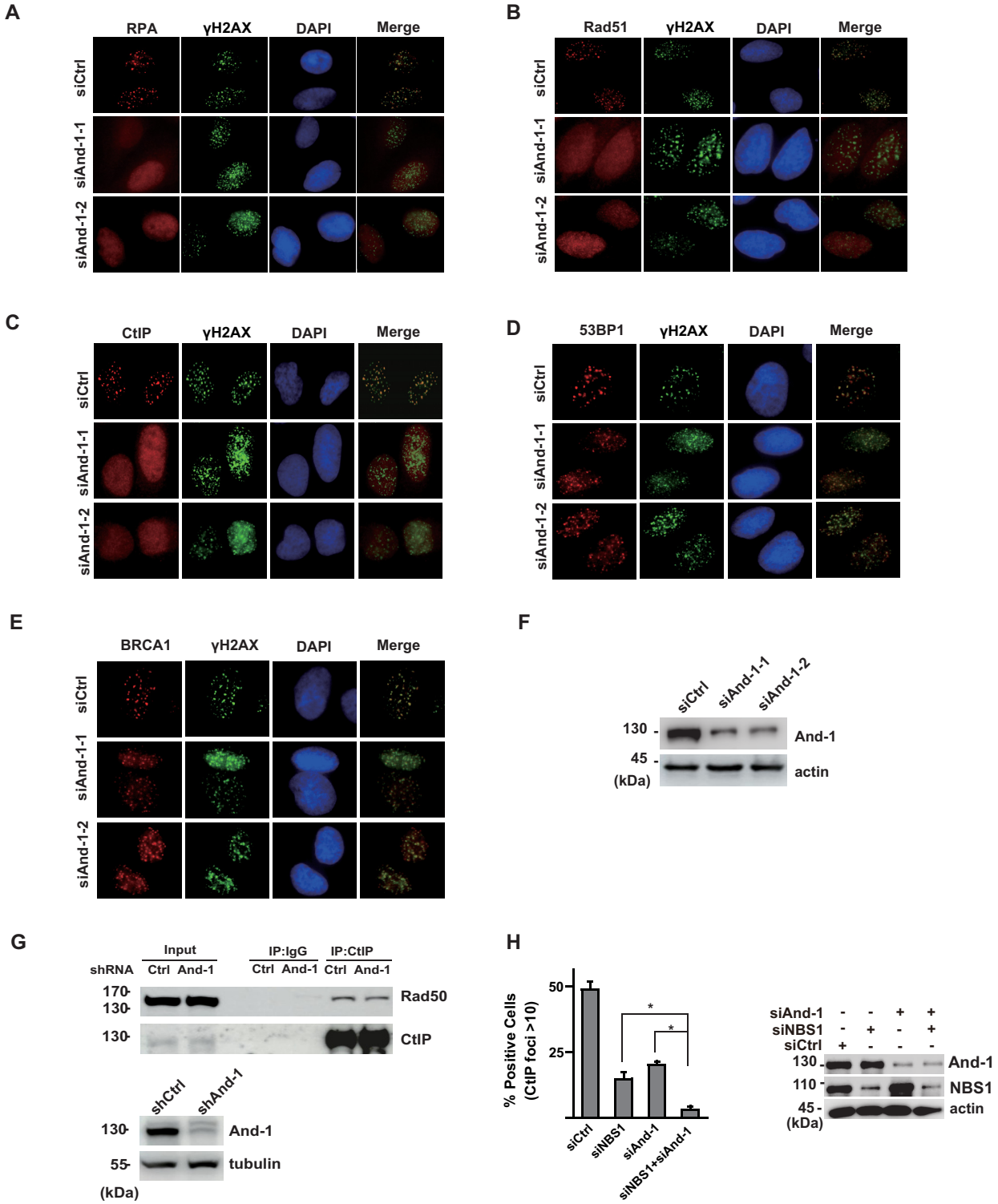

Figure 4. And-1 regulates DNA end resection. (**A**) And-1 regulates RPA IRIF. RPA and γH2AX foci formation were examined in U2OS cells transfected with control or And-1 siRNA following IR (10 Gy) treatment and a 4-h recovery. (**B** and **C**) And-1 regulates Rad51 and CtIP IRIF. Rad51(B) or CtIP(C) and γH2AX foci formation were examined in U2OS cells transfected with control or And-1 siRNA following IR (10 Gy) treatment and a 4-h recovery. (**D** and **E**) And-1 doesn't regulate 53BP1 and BRCA1 IRIF. 53BP1(D) or BRCA1(E) and γH2AX foci formation were examined in U2OS cells transfected with control or And-1 siRNA following IR (10 Gy) treatment and a 1-h recovery. (**F**) Knock-down efficiency of And-1 siRNA was examined. (**G**) And-1 doesn't influence the interaction of CtIP and the MRN complex. U2OS cells infected with control or And-1 shRNA lentivirus were synchronized to S/G2 phase, then subjected to IR (10 Gy) treatment and 1-h recovery. The cell lysates were used for Co-immunoprecipitation with the indicated antibodies. (**H**) U2OS cells were transfected with the indicated siRNAs followed by IR (10Gy) treatment and a 1-h recovery. CtIP and γH2AX foci formation was examined. Quantification, CtIP foci-posivite cells (with more than 10 foci) were counted. Total 100 cells were averaged. Data are the means of three independent experiments. Error bars represent SD. $*P < 0.05$.

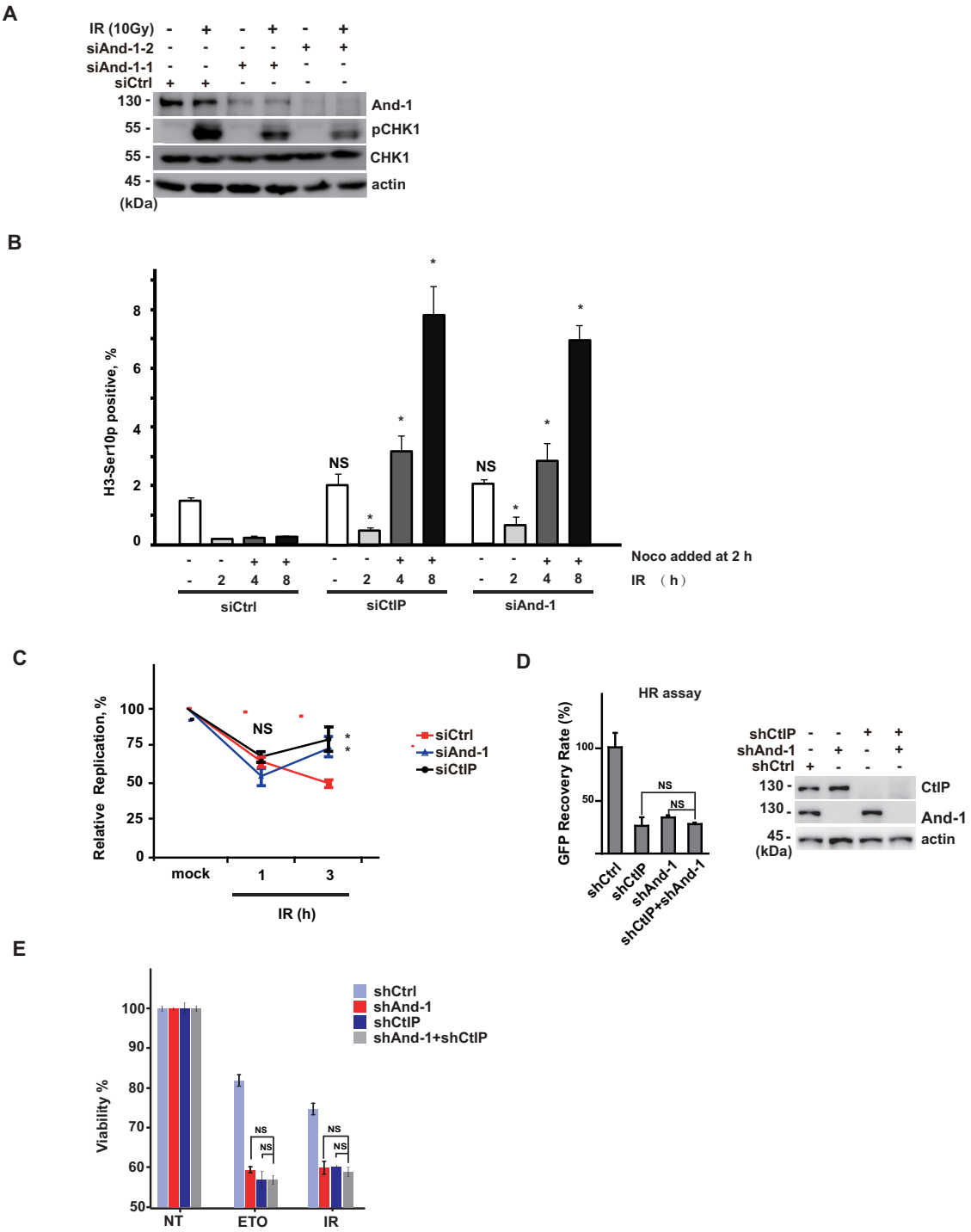

Figure 5. And-1 regulates G2/M and intra S phase checkpoint. (**A**) And-1 is required for efficient CHK1 phosphorylation in response to IR treatment. U2OS cells were transfected with the indicated siRNAs. Cells were harvested following IR(10 Gy) treatment and a 4-h recovery, and immunoblotted for the indicated proteins. (**B**) U2OS cells were transfected with the indicated siRNA for 48 h, and samples were fixed at the indicated time points after IR. And the '-' in the IR (h) label means no IR. Nocodazole (Noco) was added 2 h after IR. The bar chart shows the percentage of Histone H3-Ser10p–positive cells. H3-Ser10p–positive percentage of knockdown group was compared with control group. $*P < 0.05$. NS: no siginficant difference. Data are the means of three independent experiments. Error bars represent SDs. (**C**) RDS assay was performed using U2OS cells transfected with the indicated siRNAs. Cells were transfected for 48 h with the indicated siRNAs and subjected to RDS assay. Relative replication percentage of knockdown group was compared with control group. $*P < 0.05$. NS: no siginficant difference. Data are the means of three independent experiments. Error bars represent SDs. (**D**) HEK-293T cells integrated with HR reporter were infected with the indicated shRNA lentivirus and subjected to the HR assay as described in Methods. Data presented as mean ± SD of three biological triplicates. GFP recovery rate percentage was compared between the indicated groups. NS: no siginficant difference. (**E**) HCT116 cells were transfected with the indicated siRNAs. Sensitivity of cells to Etoposide (ETO) or IR was determined by MTS assays. Data were presented as mean ± SD of three biological triplicates. Surviving cell percentage was compared between the indicated groups. NS: no siginficant difference.

And-1 in cell cycle checkpoints. In response to irradiation, the fraction of mitotic cells in control siRNA-depleted cells was significantly reduced both at relatively early and late time points (Figure 5B). Interestingly, And-1 depleted cells did initially activate the checkpoint, as indicated by a significant decrease in mitotic cells, comparable with that of the control-depleted cells and CtIP depleted cells. However, at later time points, there was a dramatic increase in the percentage of mitotic cells in spite of irradiation, indicating a critical role for And-1 in checkpoint maintenance, which is similar as CtIP's functions (Figure 5B). Similar temporal dependency on And-1 was observed for the intra–S-phase checkpoint after IR. Initially, DNA replication was reduced in And-1-depleted cells to a level indistinguishable from control siRNA depleted cells. However, at later time points, DNA replication was substantially elevated in And-1-depleted cells relative to the control cells (Figure 5C). Based on the above results, we concluded that And-1 had the similar functions in the maintenance of checkpoint as CtIP.

Given that both And-1 and CtIP regulated DNA end resection and checkpoint maintenance, perhaps they function in the same pathway. To test this hypothesis, we double-knocked down And-1 and CtIP, then checked the HR efficiency and cell viability upon DNA damage. As shown in Figure 5D and E, double knockdown of And-1 and CtIP showed similar phenotypes (both in HR efficiency and the cell viability) as either single knockdown, and these results clearly indicate that And-1 and CtIP functions in the same pathway.

And-1-CtIP interaction is essential for DNA end resection

Since And-1 directly interacts with the N terminal of CtIP, CtIP N terminal is essential for its foci formation and knockdown of And-1 decreased CtIP foci formation, we hypothesized that And-1-CtIP interaction is required for CtIP recruitment to the DNA damage sites. To confirm this, we knocked down And-1 in U2OS cells, then reconstituted these cells with shRNA-resistant WT And-1 or the CtIP binding defficient mutant (And-1del, residues 850–1050 deleted). As shown in Figure 6A and B, WT And-1, but not And-1del, restored the HR and NHEJ efficiency. Consistent with these results, we also found that WT And-1, but not And-1del rescued the CtIP, and downstream RAD51 and RPA foci in And-1 depleted cells after IR (Figure 6C–E). These results indicating that the And-1-CtIP interaction is required for its function in DNA end resection. We also found that And-1-CtIP interaction is required for cellular resistance to DNA damage and DNA replication stress (Supplementary Figure S4A).

And-1 regulates cell cycle checkpoint through And-1-CtIP interaction

Since both And-1 and CtIP are essential for the cell cycle checkpoint after IR, we asked whether And-1-CtIP interaction is required for the checkpoint response in S and G2 phase. Again, we stably knocked down And-1 in cells using shRNA targeting the 3′-UTR region of And-1, and reconstituted cells with ectopically expressed wild type And-1 or And-1del. As shown in Figure 6F, wild type And-1, but not And-1del, restored CHK1 phosphorylation in And-1 depleted cells after IR. Consistent with these results, we also found that And-1-CtIP interaction is required for DNA damage checkpoint maintenance but not initiation (Figure 7A and B).

DISCUSSION

The tumor suppressor protein CtIP plays an important role in homologous recombination (HR)-mediated DNA double-stranded break (DSB) repair and activation of ATR and CHK1 kinases to induce the cell cycle checkpoint (8,19,35). However, how this progress is regulated has not been fully understood. Previous study showed that CtIP interacts with the MRE11-RAD50-NBS1 (MRN) complex and USP4 which is required for CtIP recruitment to DNA damage sites (19,23). Other groups also showed that BRCA1 can interact with CtIP, regulate CtIP retention at DSBs and accelerate CtIP-mediated DNA-end resection (18,20,31,58,59). BRCA1 specifically binds human CtIP isoforms that are phosphorylated at serine residue S327, primarily during the G2 phase of the cell cycle (8). But the other studies from the mouse model also showed that loss of the CtIP-BRCA1 interaction does not detectably affect resection, maintenance of genomic stability or viability (42,43). Our data provided novel insights into the molecular basis in promoting DNA-end resection. Here, we report that And-1 interacts with CtIP, which is a positive regulator of DNA end-resection, thus promoting HR (Figure 7C).

Homozygous Brca1 S1598F/S1598F mice, which express a mutant Brca1 protein defective for BRCT phospho-recognition, are prone to tumor development (60). This observation implies that the interaction of BRCA1 with one or more of its BRCT phospho-ligands is required for tumor suppression and genome stability. As above indicated, although BRCA1 BRCT domain directly binds to phosphorylated CtIP, disrupting the BRCA1-CtIP interaction does not predispose mice to tumor formation. Perhaps one or more of the other BRCT phospho-ligands functions in this process. We found that MDC1–RNF8–BRCA1 pathway affected And-1 recruitment, and BRCA1 BRCT domain was essential for And-1 recruitment, but BRCA1 BRCT domain did not directly bind And-1. Perhaps there exist other factors interacting with both BRCA1 BRCT domain and And-1. In this regard, it will be interesting to test whether BRCA1-mediated tumor suppression is affected by specific disruption of the BRCA1–Abraxas (61,62) and/or other interactions. Previous study also showed that And-1 is phosphorylated at T826 by ATR, which is required for enhanced And-1–Claspin interaction in cells with replication stress (51), but we found that And-1 T826 phosphorylation had no significant functions in And-1 recruitment or DNA end resection upon DNA double strand break (data not shown). Perhaps And-1 has different regulation mechanisms upon different genome stress. How And-1 is recruited to DSB, still needs further investigation, perhaps BRCA1 can bind an unknown protein through its BRCT domain, then the unknown protein recruits And-1.

Previous studies showed that the acidic nucleoplasmic DNA-binding protein 1 (And-1) is a replisome component and is required for efficient DNA replication in normal

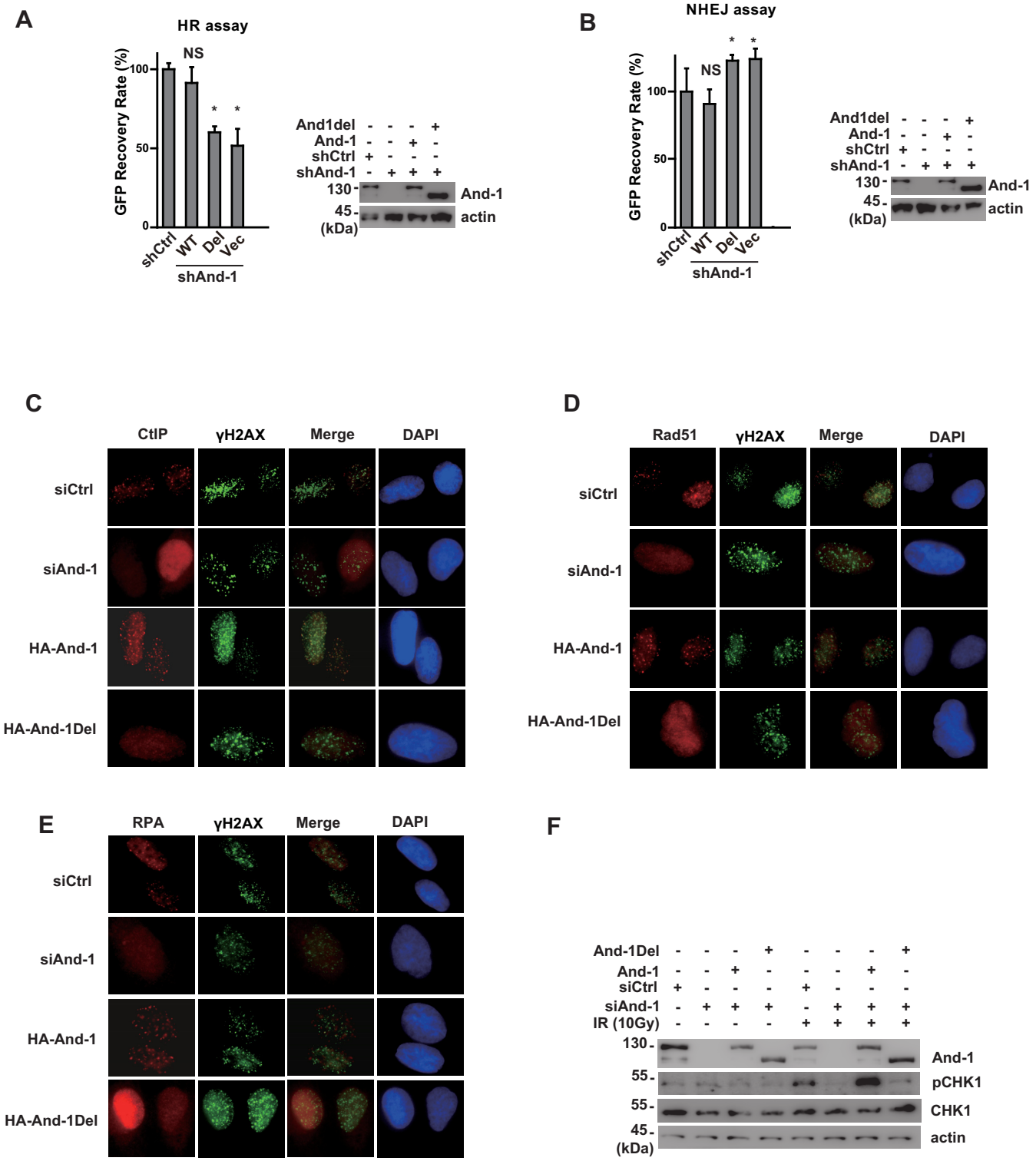

Figure 6. And-1 regulates HR through its interaction with CtIP. (**A** and **B**) HEK-293T cells integrated with HR or NHEJ reporter were infected with the indicated shRNA lentivirus and reconstituted with the indicated constructs were subjected to HR assay (A) and NHEJ assay (B) as described in Methods. GFP recovery rate percentage was compared with control group. $*P < 0.05$. NS: no siginficant difference. Data were presented as the mean ±SD of 3 independent experiments. (**C**-**E**) U2OS cells were transfected with control or And-1 siRNA, or transfected with And-1 siRNA then reconstituted with indicated siRNA-resistant WT And-1 or And-1del mutant. CtIP(C) or Rad51(D) or RPA(E) and γH2AX foci formation were examined following IR (10 Gy) treatment and a 4-h recovery. (**F**) U2OS cells infected with control or And-1 shRNA lentivirus, or reconstituted with the indicated shRNA-resistant WT And-1 or And-1del mutant. Cells were harvested following IR (10 Gy) treatment and a 2-h recovery, and immunoblotted for the indicated proteins.

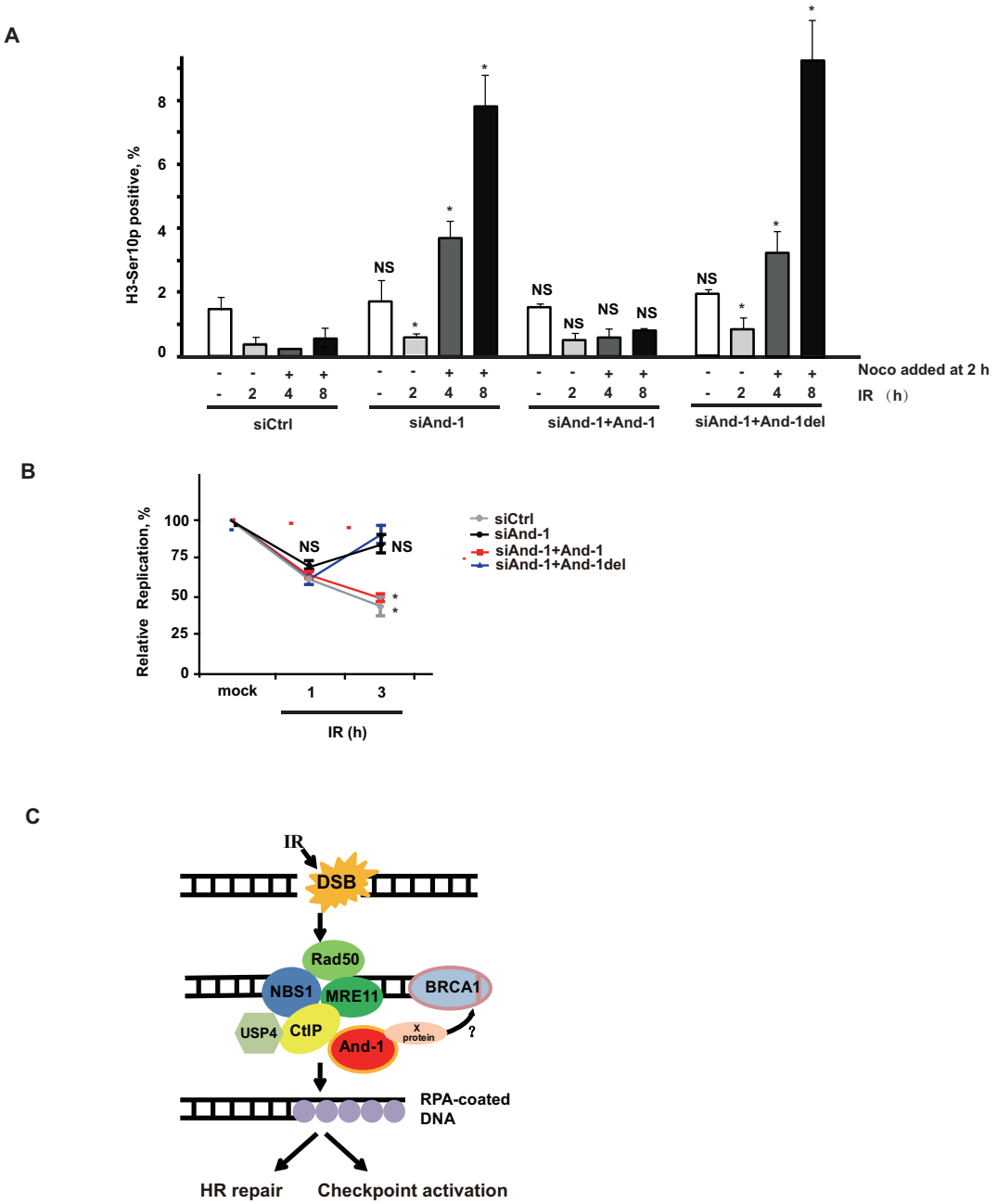

Figure 7. And-1 regulates cell cycle checkpoint through And-1-CtIP interaction. (**A**) U2OS cells were transfected with the indicated constructs for 48 h, and samples were fixed at the indicated time points after IR. Nocodazole (Noco) was added 2 h after IR. The bar chart shows the percentage of Histone H3-Ser10p–positive cells. H3-Ser10p–positive percentage was compared with control group. *$P < 0.05$. NS: no siginficant difference. Data are the means of three independent experiments. Error bars represent SDs. (**B**) RDS assay was performed using U2OS cells transfected with the indicated constructs. Cells were transfected for 48 h and subjected to RDS assay. Relative replication percentage was compared with control group. *$P < 0.05$. NS: no siginficant difference. Data are the means of three independent experiments. Error bars represent SDs. (**C**) A working model demonstrating how And-1 regulates double-strand break end resection and DNA damage checkpoint maintenance.

and tumour cells (44,46,63–67). Ctf4/Mcl1, the ortholog of And-1 in yeast, is required for chromosome transmission fidelity, sister chromatin cohesion, DNA damage repair, maintenance of genome integrity, and the regulation of telomere replication (68–70). Recent studies indicate that And-1 coordinates with claspin in response to replication stress. Here, we have identified, for the first time, a novel CtIP–And-1 functional link that directly functions in DNA end resection during HR and chemotherapy drug response. For example, similar to CtIP depletion, And-1 depletion rendered cells hypersensitive to many chemotherapy drugs, such as Etoposide and PARP inhibitor (AZD2281) (Figure 3D), which have been used in clinical for patients with breast, ovarian and prostate cancer. It is thus, timely to evaluate the potential for And-1 as DDR drug targets for therapeutic intervention. The synthetic lethal approach provides

exciting opportunities for therapeutic targeting of cancers exhibiting high levels of DNA damage or which have underlying defects in DDR processes or chromatin components.

In summary, our work indicates that And-1 is a critical factor in the maintenance of genome stability through HR-dependent repair of DSBs, including those induced by commonly used anticancer agents, such as IR or Etoposide. This will provide new strategies for the development of highly specific anti-cancer therapies targeting And-1 or And-1-dependent processes.

SUPPLEMENTARY DATA

Supplementary Data are available at NAR Online.

ACKNOWLEDGMENTS

We thank all colleagues in Dr Huadong Pei's laboratory for insightful discussions and technical assistance. We thank Dr Wenge Zhu at The George Washington University Medical School for providing the pEFF-And-1 construct and the homemade And-1 antibody. We thank Dr Hailong Wang at Capital Normal University for providing the GFP-CtIP plasmid. We thank Gr. Stark, J. M at Beckman Research Institute of the City of Hope for generously providing the intergrated DNA repair reporter system. We thank the Imaging Facility of National Center for Protein Sciences-Beijing (NCPSB) for assistance with Microscopy imaging and image data analysis.

FUNDING

National Basic Research Program of China 973 Program]2015CB910600 and 2013CB910300]; National Natural Science Foundation of China [31371433, 31571463, 81572740 and 31301123]; International S&T Cooperation Program of China [2015DFA31680 and 2015DFA30610]; State Key Laboratory of Proteomics [SKLP-O201303]; One Thousand Young Talent Program (to H.D.P.). Funding for open access charge: National Basic Research Program of China 973 Program [2015CB910600].
Conflict of interest statement. None declared.

REFERENCES

1. Ciccia,A. and Elledge,S.J. (2010) The DNA damage response: making it safe to play with knives. *Mol. Cell*, **40**, 179–204.
2. Friedberg,E.C., Aguilera,A., Gellert,M., Hanawalt,P.C., Hays,J.B., Lehmann,A.R., Lindahl,T., Lowndes,N., Sarasin,A. and Wood,R.D. (2006) DNA repair: from molecular mechanism to human disease. *DNA Repair*, **5**, 986–996.
3. Jackson,S.P. and Bartek,J. (2009) The DNA-damage response in human biology and disease. *Nature*, **461**, 1071–1078.
4. Cimprich,K.A. and Cortez,D. (2008) ATR: an essential regulator of genome integrity. *Nat. Rev. Mol. Cell Biol.*, **9**, 616–627.
5. Harper,J.W. and Elledge,S.J. (2007) The DNA damage response: ten years after. *Mol. Cell*, **28**, 739–745.
6. Jeggo,P.A., Pearl,L.H. and Carr,A.M. (2016) DNA repair, genome stability and cancer: a historical perspective. *Nat. Rev. Cancer*, **16**, 35–42.
7. Polo,S.E. and Jackson,S.P. (2011) Dynamics of DNA damage response proteins at DNA breaks: a focus on protein modifications. *Genes Dev.*, **25**, 409–433.
8. Yu,X. and Chen,J. (2004) DNA damage-induced cell cycle checkpoint control requires CtIP, a phosphorylation-dependent binding partner of BRCA1 C-terminal domains. *Mol. Cell. Biol.*, **24**, 9478–9486.
9. Medema,R.H. and Macurek,L. (2012) Checkpoint control and cancer. *Oncogene*, **31**, 2601–2613.
10. Shaltiel,I.A., Krenning,L., Bruinsma,W. and Medema,R.H. (2015) The same, only different - DNA damage checkpoints and their reversal throughout the cell cycle. *J. Cell Sci.*, **128**, 607–620.
11. Lieber,M.R. (2010) The mechanism of double-strand DNA break repair by the nonhomologous DNA end-joining pathway. *Annu. Rev. Biochem.*, **79**, 181–211.
12. San Filippo,J., Sung,P. and Klein,H. (2008) Mechanism of eukaryotic homologous recombination. *Annu. Rev. Biochem.*, **77**, 229–257.
13. Wyman,C. and Kanaar,R. (2006) DNA double-strand break repair: all's well that ends well. *Annu. Rev. Genet.*, **40**, 363–383.
14. Lee,J.H. and Paull,T.T. (2005) ATM activation by DNA double-strand breaks through the Mre11-Rad50-Nbs1 complex. *Science*, **308**, 551–554.
15. Rupnik,A., Lowndes,N.F. and Grenon,M. (2010) MRN and the race to the break. *Chromosoma*, **119**, 115–135.
16. Garcia,V., Phelps,S.E., Gray,S. and Neale,M.J. (2011) Bidirectional resection of DNA double-strand breaks by Mre11 and Exo1. *Nature*, **479**, 241–244.
17. Paull,T.T. (2015) Mechanisms of ATM Activation. *Annu. Rev. Biochem.*, **84**, 711–738.
18. Chen,L., Nievera,C.J., Lee,A.Y. and Wu,X. (2008) Cell cycle-dependent complex formation of BRCA1.CtIP.MRN is important for DNA double-strand break repair. *J. Biol. Chem.*, **283**, 7713–7720.
19. Sartori,A.A., Lukas,C., Coates,J., Mistrik,M., Fu,S., Bartek,J., Baer,R., Lukas,J. and Jackson,S.P. (2007) Human CtIP promotes DNA end resection. *Nature*, **450**, 509–514.
20. Yun,M.H. and Hiom,K. (2009) CtIP-BRCA1 modulates the choice of DNA double-strand-break repair pathway throughout the cell cycle. *Nature*, **459**, 460–463.
21. Takeda,S., Nakamura,K., Taniguchi,Y. and Paull,T.T. (2007) Ctp1/CtIP and the MRN complex collaborate in the initial steps of homologous recombination. *Mol. Cell*, **28**, 351–352.
22. Makharashvili,N. and Paull,T.T. (2015) CtIP: A DNA damage response protein at the intersection of DNA metabolism. *DNA Repair*, **32**, 75–81.
23. Liu,H., Zhang,H., Wang,X., Tian,Q., Hu,Z., Peng,C., Jiang,P., Wang,T., Guo,W., Chen,Y. *et al.* (2015) The deubiquitylating enzyme USP4 cooperates with CtIP in DNA double-strand break end resection. *Cell Rep.*, **13**, 93–107.
24. Wijnhoven,P., Konietzny,R., Blackford,A.N., Travers,J., Kessler,B.M., Nishi,R. and Jackson,S.P. (2015) USP4 auto-deubiquitylation promotes homologous recombination. *Mol. Cell*, **60**, 362–373.
25. Broderick,R., Nieminuszczy,J., Baddock,H.T., Deshpande,R.A., Gileadi,O., Paull,T.T., McHugh,P.J. and Niedzwiedz,W. (2016) EXD2 promotes homologous recombination by facilitating DNA end resection. *Nat. Cell Biol.*, **18**, 271–280.
26. Hopkins,B.B. and Paull,T.T. (2008) The P. furiosus mre11/rad50 complex promotes 5′ strand resection at a DNA double-strand break. *Cell*, **135**, 250–260.
27. Nimonkar,A.V., Genschel,J., Kinoshita,E., Polaczek,P., Campbell,J.L., Wyman,C., Modrich,P. and Kowalczykowski,S.C. (2011) BLM-DNA2-RPA-MRN and EXO1-BLM-RPA-MRN constitute two DNA end resection machineries for human DNA break repair. *Genes Dev.*, **25**, 350–362.
28. Shibata,A., Moiani,D., Arvai,A.S., Perry,J., Harding,S.M., Genois,M.M., Maity,R., van Rossum-Fikkert,S., Kertokalio,A., Romoli,F. *et al.* (2014) DNA double-strand break repair pathway choice is directed by distinct MRE11 nuclease activities. *Mol. Cell*, **53**, 7–18.
29. Wu,Y., Lee,S.H., Williamson,E.A., Reinert,B.L., Cho,J.H., Xia,F., Jaiswal,A.S., Srinivasan,G., Patel,B., Brantley,A. *et al.* (2015) EEPD1 rescues stressed replication forks and maintains genome stability by promoting end resection and homologous recombination repair. *PLoS Genet.*, **11**, e1005675.
30. Zhu,Z., Chung,W.H., Shim,E.Y., Lee,S.E. and Ira,G. (2008) Sgs1 helicase and two nucleases Dna2 and Exo1 resect DNA double-strand break ends. *Cell*, **134**, 981–994.
31. Makharashvili,N., Tubbs,A.T., Yang,S.H., Wang,H., Barton,O., Zhou,Y., Deshpande,R.A., Lee,J.H., Lobrich,M., Sleckman,B.P. *et al.*

(2014) Catalytic and noncatalytic roles of the CtIP endonuclease in double-strand break end resection. *Mol. Cell*, **54**, 1022–1033.
32. Wang,H., Li,Y., Truong,L.N., Shi,L.Z., Hwang,P.Y., He,J., Do,J., Cho,M.J., Li,H., Negrete,A. *et al.* (2014) CtIP maintains stability at common fragile sites and inverted repeats by end resection-independent endonuclease activity. *Mol. Cell*, **54**, 1012–1021.
33. Marechal,A. and Zou,L. (2015) RPA-coated single-stranded DNA as a platform for post-translational modifications in the DNA damage response. *Cell Res.*, **25**, 9–23.
34. Zou,L. and Elledge,S.J. (2003) Sensing DNA damage through ATRIP recognition of RPA-ssDNA complexes. *Science*, **300**, 1542–1548.
35. Kousholt,A.N., Fugger,K., Hoffmann,S., Larsen,B.D., Menzel,T., Sartori,A.A. and Sorensen,C.S. (2012) CtIP-dependent DNA resection is required for DNA damage checkpoint maintenance but not initiation. *J. Cell Biol.*, **197**, 869–876.
36. You,Z. and Bailis,J.M. (2010) DNA damage and decisions: CtIP coordinates DNA repair and cell cycle checkpoints. *Trends Cell Biol.*, **20**, 402–409.
37. Smits,V.A. and Gillespie,D.A. (2015) DNA damage control: regulation and functions of checkpoint kinase 1. *FEBS J.*, **282**, 3681–3692.
38. Ferretti,L.P., Lafranchi,L. and Sartori,A.A. (2013) Controlling DNA-end resection: a new task for CDKs. *Front. Genet.*, **4**, 99.
39. Huertas,P. and Jackson,S.P. (2009) Human CtIP mediates cell cycle control of DNA end resection and double strand break repair. *J. Biol. Chem.*, **284**, 9558–9565.
40. Escribano-Diaz,C., Orthwein,A., Fradet-Turcotte,A., Xing,M., Young,J.T., Tkac,J., Cook,M.A., Rosebrock,A.P., Munro,M., Canny,M.D. *et al.* (2013) A cell cycle-dependent regulatory circuit composed of 53BP1-RIF1 and BRCA1-CtIP controls DNA repair pathway choice. *Mol.Cell*, **49**, 872–883.
41. Escribano-Diaz,C. and Durocher,D. (2013) DNA repair pathway choice—a PTIP of the hat to 53BP1. *EMBO Rep.*, **14**, 665–666.
42. Reczek,C.R., Szabolcs,M., Stark,J.M., Ludwig,T. and Baer,R. (2013) The interaction between CtIP and BRCA1 is not essential for resection-mediated DNA repair or tumor suppression. *J. Cell Biol.*, **201**, 693–707.
43. Polato,F., Callen,E., Wong,N., Faryabi,R., Bunting,S., Chen,H.T., Kozak,M., Kruhlak,M.J., Reczek,C.R., Lee,W.H. *et al.* (2014) CtIP-mediated resection is essential for viability and can operate independently of BRCA1. *J. Exp. Med.*, **211**, 1027–1036.
44. Zhu,W., Ukomadu,C., Jha,S., Senga,T., Dhar,S.K., Wohlschlegel,J.A., Nutt,L.K., Kornbluth,S. and Dutta,A. (2007) Mcm10 and And-1/CTF4 recruit DNA polymerase alpha to chromatin for initiation of DNA replication. *Genes Dev.*, **21**, 2288–2299.
45. Jaramillo-Lambert,A., Hao,J., Xiao,H., Li,Y., Han,Z. and Zhu,W. (2013) Acidic nucleoplasmic DNA-binding protein (And-1) controls chromosome congression by regulating the assembly of centromere protein A (CENP-A) at centromeres. *J. Biol. Chem.*, **288**, 1480–1488.
46. Im,J.S., Ki,S.H., Farina,A., Jung,D.S., Hurwitz,J. and Lee,J.K. (2009) Assembly of the Cdc45-Mcm2-7-GINS complex in human cells requires the Ctf4/And-1, RecQL4, and Mcm10 proteins. *Proc. Natl. Acad. Sci. U.S.A.*, **106**, 15628–15632.
47. Lou,Z., Minter-Dykhouse,K., Wu,X. and Chen,J. (2003) MDC1 is coupled to activated CHK2 in mammalian DNA damage response pathways. *Nature*, **421**, 957–961.
48. Luo,K., Zhang,H., Wang,L., Yuan,J. and Lou,Z. (2012) Sumoylation of MDC1 is important for proper DNA damage response. *EMBO J.*, **31**, 3008–3019.
49. Pei,H., Zhang,L., Luo,K., Qin,Y., Chesi,M., Fei,F., Bergsagel,P.L., Wang,L., You,Z. and Lou,Z. (2011) MMSET regulates histone H4K20 methylation and 53BP1 accumulation at DNA damage sites. *Nature*, **470**, 124–128.
50. Yuan,J. and Chen,J. (2009) N terminus of CtIP is critical for homologous recombination-mediated double-strand break repair. *J. Biol. Chem.*, **284**, 31746–31752.
51. Hao,J., de Renty,C., Li,Y., Xiao,H., Kemp,M.G., Han,Z., DePamphilis,M.L. and Zhu,W. (2015) And-1 coordinates with Claspin for efficient Chk1 activation in response to replication stress. *EMBO J.*, **34**, 2096–2110.
52. Manke,I.A., Lowery,D.M., Nguyen,A. and Yaffe,M.B. (2003) BRCT repeats as phosphopeptide-binding modules involved in protein targeting. *Science*, **302**, 636–639.
53. Yu,X., Chini,C.C., He,M., Mer,G. and Chen,J. (2003) The BRCT domain is a phospho-protein binding domain. *Science*, **302**, 639–642.
54. Rodriguez,M., Yu,X., Chen,J. and Songyang,Z. (2003) Phosphopeptide binding specificities of BRCA1 COOH-terminal (BRCT) domains. *J. Biol. Chem.*, **278**, 52914–52918.
55. Chapman,J.R., Barral,P., Vannier,J.B., Borel,V., Steger,M., Tomas-Loba,A., Sartori,A.A., Adams,I.R., Batista,F.D. and Boulton,S.J. (2013) RIF1 is essential for 53BP1-dependent nonhomologous end joining and suppression of DNA double-strand break resection. *Mol. Cell*, **49**, 858–871.
56. Fattah,F., Lee,E.H., Weisensel,N., Wang,Y., Lichter,N. and Hendrickson,E.A. (2010) Ku regulates the non-homologous end joining pathway choice of DNA double-strand break repair in human somatic cells. *PLoS Genet.*, **6**, e1000855.
57. Stauffer,M.E. and Chazin,W.J. (2004) Physical interaction between replication protein A and Rad51 promotes exchange on single-stranded DNA. *J. Biol. Chem.*, **279**, 25638–25645.
58. Cruz-Garcia,A., Lopez-Saavedra,A. and Huertas,P. (2014) BRCA1 accelerates CtIP-mediated DNA-end resection. *Cell Rep.*, **9**, 451–459.
59. Yu,X., Fu,S., Lai,M., Baer,R. and Chen,J. (2006) BRCA1 ubiquitinates its phosphorylation-dependent binding partner CtIP. *Genes Dev.*, **20**, 1721–1726.
60. Shakya,R., Reid,L.J., Reczek,C.R., Cole,F., Egli,D., Lin,C.S., deRooij,D.G., Hirsch,S., Ravi,K., Hicks,J.B. *et al.* (2011) BRCA1 tumor suppression depends on BRCT phosphoprotein binding, but not its E3 ligase activity. *Science*, **334**, 525–528.
61. Wang,B., Matsuoka,S., Ballif,B.A., Zhang,D., Smogorzewska,A., Gygi,S.P. and Elledge,S.J. (2007) Abraxas and RAP80 form a BRCA1 protein complex required for the DNA damage response. *Science*, **316**, 1194–1198.
62. Castillo,A., Paul,A., Sun,B., Huang,T.H., Wang,Y., Yazinski,S.A., Tyler,J., Li,L., You,M.J., Zou,L. *et al.* (2014) The BRCA1-interacting protein Abraxas is required for genomic stability and tumor suppression. *Cell Rep.*, **8**, 807–817.
63. Errico,A., Cosentino,C., Rivera,T., Losada,A., Schwob,E., Hunt,T. and Costanzo,V. (2009) Tipin/Tim1/And1 protein complex promotes Pol alpha chromatin binding and sister chromatid cohesion. *The EMBO J.*, **28**, 3681–3692.
64. Gambus,A., van Deursen,F., Polychronopoulos,D., Foltman,M., Jones,R.C., Edmondson,R.D., Calzada,A. and Labib,K. (2009) A key role for Ctf4 in coupling the MCM2-7 helicase to DNA polymerase alpha within the eukaryotic replisome. *EMBO J.*, **28**, 2992–3004.
65. Yoshizawa-Sugata,N. and Masai,H. (2009) Roles of human AND-1 in chromosome transactions in S phase. *J. Biol. Chem.*, **284**, 20718–20728.
66. Bermudez,V.P., Farina,A., Tappin,I. and Hurwitz,J. (2010) Influence of the human cohesion establishment factor Ctf4/AND-1 on DNA replication. *J. Biol. Chem.*, **285**, 9493–9505.
67. Li,Y., Jaramillo-Lambert,A.N., Yang,Y., Williams,R., Lee,N.H. and Zhu,W. (2012) And-1 is required for the stability of histone acetyltransferase Gcn5. *Oncogene*, **31**, 643–652.
68. Mayer,M.L., Pot,I., Chang,M., Xu,H., Aneliunas,V., Kwok,T., Newitt,R., Aebersold,R., Boone,C., Brown,G.W. *et al.* (2004) Identification of protein complexes required for efficient sister chromatid cohesion. *Mol. Biol. Cell*, **15**, 1736–1745.
69. Samora,C.P., Saksouk,J., Goswami,P., Wade,B.O., Singleton,M.R., Bates,P.A., Lengronne,A., Costa,A. and Uhlmann,F. (2016) Ctf4 links DNA replication with sister chromatid cohesion establishment by recruiting the Chl1 helicase to the replisome. *Mol. Cell*, **63**, 371–384.
70. Villa,F., Simon,A.C., Ortiz Bazan,M.A., Kilkenny,M.L., Wirthensohn,D., Wightman,M., Matak-Vinkovic,D., Pellegrini,L. and Labib,K. (2016) Ctf4 is a hub in the eukaryotic replisome that links multiple CIP-box proteins to the CMG helicase. *Mol. Cell*, **63**, 385–396.